Research Article Vol. 29, No. 2 / 18 January 2021 / Optics Express 2679
Optics EXPRESS

Realization of compact Watt-level single-frequency continuous-wave self-tuning titanium: sapphire laser

JIAO WEI,[1] XUECHEN CAO,[1] PIXIAN JIN,[1,2] ZHU SHI,[1,2] JING SU,[1,2] AND HUADONG LU[1,2,*]

[1]State Key Laboratory of Quantum Optics and Quantum Optics Devices, Institute of Opto-Electronics, Shanxi University, Taiyuan 030006, China
[2]Collaborative Innovation Center of extreme Optics, Shanxi University, Taiyuan 030006, China
[*]luhuadong@sxu.edu.cn

Abstract: Here, we present a compact Watt-level single-frequency continuous-wave (CW) self-tuning titanium:sapphire (Ti:S) laser, which is implemented using a three-plate Ti:S crystal as both a gain medium and frequency-tuning element. The thickness ratio of the three-plate Ti:S crystal is 1:2:4, of which the thinnest plate measured 1 mm. The optical axes lie on their own surfaces and parallel to each other. Based on the presented self-tuning crystal, a ring resonator is designed and built. The maximum wavelength tuning range of the single-frequency self-tuning Ti:S laser is 108.84 nm, as demonstrated experimentally by rotating the three-plate Ti:S crystal, indicating good agreement with theoretical prediction. To the best of our knowledge, this is the first study to report a single-frequency CW self-tuning Ti:S laser, which can provide a feasible approach for achieving a compact all-solid-state single-frequency CW-tunable Ti:S laser.

© 2021 Optical Society of America under the terms of the OSA Open Access Publishing Agreement

1. Introduction

All-solid-state single-frequency continuous-wave (CW) tunable titanium:sapphire (Ti:S) laser [1] has been applied in atomic physics [2–4], quantum communication [5], and precise measurements [6] owing to its intrinsic advantages including low intensity noise, perfect beam quality, high stability, and broad tuning range in particular. The first room-temperature CW Ti:S laser was reported in 1986 [7], and it provided a function for the development of practical Ti:S lasers at room temperature. Subsequently, P. A. Schulz realized a single-frequency CW-tunable Ti:S laser with a wavelength tuning range of 100 nm [8]. With the development of frequency-doubled Nd-doped lasers pumped by a laser diode, all-solid-state single-frequency Ti:S lasers [9] have become increasingly popular because of their compactness, high efficiency and long life. To date, five types of commercial all-solid-state single-frequency CW-tunable Ti:S lasers are available, and they are produced by M-square [10], Coherent [11], Spectra-Physics [12], Tekhnoscan Joint-Stock [13], and Shanxi University [14,15]. To achieve broad and continuous frequency tuning in these single-frequency CW-tunable Ti:S lasers, a multi-plate quartz birefringent filter (BRF), a locked etalon (E) and a broadband optical diode (OD) must be employed in the resonator. However, intracavity elements significantly increase the insertion loss and further decrease the optical conversion efficiency. In 2017, our group developed a new self-injection-locked single-frequency tunable Ti:S laser, which was implemented by replacing a broadband OD with a broadband retro-reflecting device to achieve a stable unidirectional operation of Ti:S laser. In this case, the intracavity loss was decreased effectively, and the output power was improved from 2.88 to 5.0 W [16]. That study provided a method to further decrease the intracavity elements of a Ti:S laser. Additionally, in 2003, Fernandez experimentally demonstrated broadband wavelength self-tuning in a $K_5Nd(MoO_4)_4$ crystal for the first time, providing an effective method for realize a compact tunable laser [17]. Subsequently, the method developed by Fernandez was quickly extended to

#415873 https://doi.org/10.1364/OE.415873
Journal © 2021 Received 25 Nov 2020; revised 1 Jan 2021; accepted 4 Jan 2021; published 14 Jan 2021

Optics EXPRESS

other self-tuning lasers including $Rb_5Nd(MoO_4)_4$, $La_3Ga_5SiO_{14}$:Nd^{3+}, and Ti:S laser [18,19]. In 2005, Iparraguirre et al. realized a self-tuning Ti:S pulsed laser with a tuning range of 120 nm by adopting a single-plate Ti:S crystal [20]. Subsequently, they further expanded the tuning range of the self-tuning Ti:S laser to 250 nm by employing a three-plate Ti:S crystal in 2009 [21]. However, reports regarding single-frequency CW self-tuning lasers do not exist, to the best of our knowledge. This paper is the first to report, a compact Watt-level single-frequency CW self-tuning Ti:S laser, which was implemented using a three-plate Ti:S crystal as both the gain medium and frequency-tuning element. The thickness ratio of the three-plate Ti:S crystal was 1:2:4, of which the thinnest plate measured 1 mm. The optical axes were positioned on their own surfaces and parallel to each other. When the laser resonator was optimized to compensate for the astigmatism caused by the Brewster angle incident elements and the thermal effect, a compact Watt-level single-frequency self-tuning Ti:S laser with a maximum wavelength tuning range of 108.84 nm was obtained.

2. Theoretical analysis

Ti:S crystal is a type of birefringent crystal and an excellent laser material owing to its simple energy-level structure, broad tuning range, good thermal conductivity and relatively large gain cross section. As shown in Fig. 1(a), the traditional Ti:S crystal is cut into sticks, and both ends of the rod are cut at the Brewster angle (60.4°). The polarization of the pump light ($\sum(k)$) transmitted at the Brewster angle face is in the direction of the optical axes $\sum(c)$. The polarization of the pump light along the c-axis provides the highest absorption in the blue-green region, and the highest emission in the infrared range. However, once the crystal rotates around the x-axis, the angle between the optical axes $\sum(c)$ and the polarization direction of the incident light changes continuously, thereby directly inducing the wavelength variations in the transmitted laser based on polarization interference tuning theory. In this case, the filtering effect of the rotatable Ti:S crystal is the same as that of the traditional BRF. For the Ti:S crystal, the refractive indices of the ordinary (o) and extraordinary (e) light are n_o=1.762 and n_e=1.770, the refractive index difference was 0.008, which was slightly smaller than that (0.01) of the quartz crystal [22]. Therefore, the Ti:S crystal can serve as both a frequency selection element and gain medium.

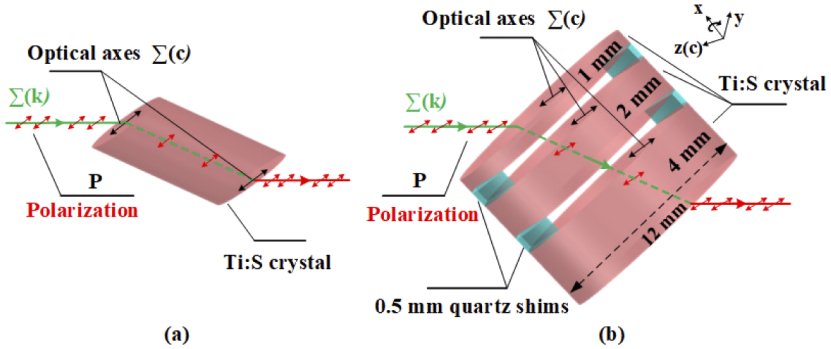

Fig. 1. Diagrams of (a) traditional Ti:S crystal, (b) designed three-plate Ti:S crystal in single-frequency CW tunable Ti:S laser.

A rotatable three-plate Ti:S crystal termed "self-tuning crystal (STC)" was experimentally designed, and its parameters are shown in Fig.1(b). It is composed of three Ti:S crystal plates and four quartz shims. The thickness ratio of the three-plate Ti:S crystal was 1:2:4, of which the thinnest plate measured 1 mm by considering the processing difficulty of the single-plate Ti:S crystal and the tuning ability. The thickness of the four crescent quartz shims was manufactured

Optics EXPRESS

to be 0.5 mm. The optical axes $\sum(c)$ were positioned on their own surfaces and parallel to each other, and their directions were denoted using quartz shims. In addition, considering that the total thickness of the STC was 8 mm, the diameter was customized to 12 mm to ensure the easy propagation of the pump laser.

The operating wavelength as a function of the tuning angle φ (the angle between the optical axes and the incident plane) can be expressed as

$$\lambda = \frac{d_i}{k}\left[n_e\sqrt{1-\sin^2\theta\left(\frac{\sin^2\varphi}{n_e^2}+\frac{\sin^2\varphi}{n_o^2}\right)}-n_o\sqrt{1-\frac{\sin^2\theta}{n_o^2}}\right], \tag{1}$$

where d_i (i=1, 2, 3) is the thickness of the Ti:S crystal plate; k is the interference order; n_o and n_e are the refractive indices of the "o" and "e" light, respectively; θ is the incident angle, which was set as the Brewster angle in the experiment. Subsequently, the transmission of the STC is expressed as follows:

$$T = \prod_{i=1}^{i=3}\left[1-\sin^2\varphi\frac{n_o^4-n_o^2\cos^2\theta}{n_o^2-\cos^2\theta\cos^2\varphi}\sin^2\left[\frac{\pi d_i}{\lambda}\left(n_e\frac{1+\frac{\cos^2\theta\cos^2\varphi}{n_e^2}-\frac{\cos^2\theta\cos^2\varphi}{n_o^2}}{\sqrt{1-\cos^2\theta\left(\frac{\sin^2\varphi}{n_e^2}+\frac{\cos^2\varphi}{n_o^2}\right)}}-\frac{n_o}{\sqrt{1-\frac{\cos^2\theta}{n_o^2}}}\right)\right]\right]. \tag{2}$$

Using Eqs.(1) and (2), the tuning and transmission curves of the designed STC were theoretically simulated and plotted, as shown in Fig. 2 and 3, respectively. As shown in Fig. 2, the tuning curve of k = 10 can encompass the wavelength range of 700-900 nm when the tuning angle varied from 7.5° to 72.5°, and the corresponding tuning slope efficiency was 3.1 nm/°. As shown in Fig. 3, the transmittances of the sidebands were below 6.62% at all times, revealing the capability of the designed STC in well suppressing the sidebands, and ensuring the smooth tuning of the broadband laser.

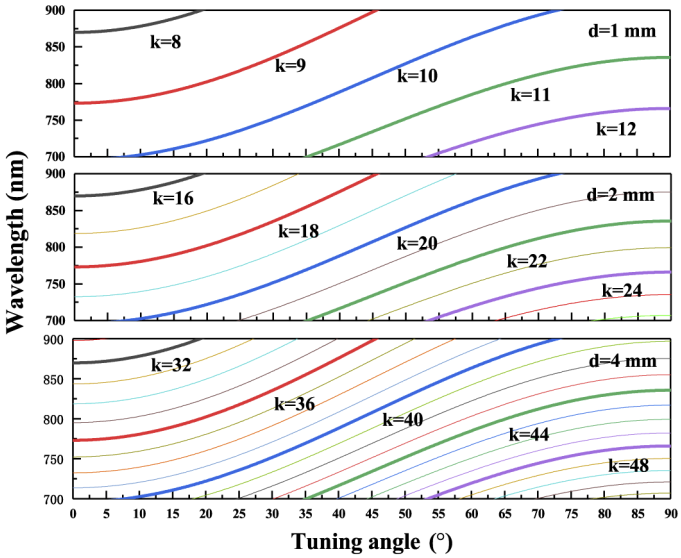

Fig. 2. Theoretical simulation of the tuning curves of the designed STC.

Optics EXPRESS

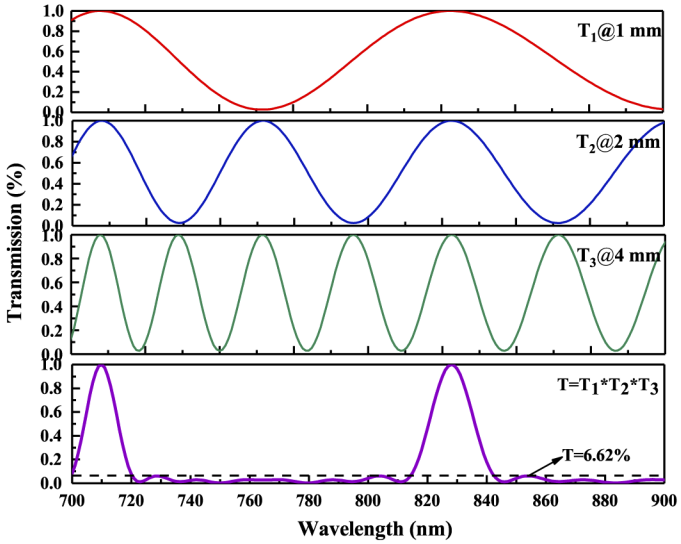

Fig. 3. Theoretical simulation of the transmission curve of the designed STC.

3. Experimental setup

Based on the designed STC, an all-solid-state single-frequency CW self-tuning Ti:S laser was experimentally built and its schematic diagram is illustrated in Fig. 4. The pump source was a high-quality all-solid-state single-frequency CW 532 nm laser with a maximum radiation power of 12.5 W (DPSS FG-VIII, Yuguang Co., Ltd.) [23–25]. The measured stability and beam quality of the pump laser were better than ±1% (peak-to-peak fluctuation) and 1.1 (M^2). The polarization of the pump laser was aligned to p-polarized using a half-wave plate. In this case, the polarization of the pump laser was parallel to the optical axis of the STC and was termed the starting point of the rotation. To achieve precise mode matching, the pump laser beam was collimated by a lens f_1 with a focal length of 200 mm and then focused into the STC with a beam waist of 48 μm by lens f_2 with a focal length of 120 mm. The bow-tie-type ring resonator comprised a concave-convex mirror M_1 (R_{convex}=-100 mm; $R_{concave}$=100 mm), a plane-concave mirror M_2 ($R_{concave}$=100 mm), and two plane mirrors M_3 and M_4. M_1 and M_2 were coated with the high transmission (HT, T_{532}<95%) film for 532 nm laser and high reflection (HR, $R_{740-890}$>99.5%) film for 740-890 nm laser. M_3 was coated with HR film ($R_{740-890}$>99.5%) for 740-890 nm laser. The output coupler M_4 was coated with the transmission of 5.5% ($T_{740-890}$=5.5%±0.5%) film for 740-890 nm laser. The STC (SIDM. Co., Ltd.) was composed of three Ti:S crystal plates and four quartz shims. The thickness ratio of the STC was 1:2:4, of which the thinnest plate meaured 1 mm. The optical axes of three Ti:S crystal plates were positioned on their own surfaces and parallel to each other, and their directions were denoted using quartz shims. The Ti^{3+} doping concentration was customized to 0.08 wt.% by considering the absorption efficiency of the pump light and the parasitic losses of the resonant light. In the experiment, to ensure the rotation precision around the x-axis and cool the STC simultaneously, the STC was mounted on a spatially adjustable oven cooled using cool circulation water at a temperature of 16°C. The crystal oven was installed on a piezoelectric rotating electrical machine (AG-PR100, Newport) to achieve precise rotation. The STC was placed at the waist between cavity mirrors M_1 and M_2 to achieve a sufficient pump rate. Because of the small pump waist and the large diameter and high doping concentration of the STC, the focal length of the induced thermal lens measured 110 mm in the experiment under a pump power of 11.5 W. Considering the thermal lens effect of the STC, the stabilization range of

Optics EXPRESS

the laser resonator and the beam waist of the STC were theoretically calculated using LaserCAD software. Consequently, the lengths between M_1 and the front face of the STC, and that between M_2 and the rear face of the STC were optimized to 48.7 and 46.3 mm, respectively. To further compensate for the astigmatism caused by the Brewster incident angle STC, the incident angles of M_1 and M_2 were both optimized to 10°. In addition, an E with a thickness of 1 mm adhering to the spindle of a galvanometer scanner (GS) was inserted into the resonator to suppress mode hops and finely tune the oscillating frequency by adjusting its incident angle. The laser beam reflected from the E was reflected again by a triangle prism and then focused into a photodetector (PD) by a focal lens (f_3=35 mm). The detected signal output from the PD was mixed with the modulation signal to extract the error signal. The generated error signal was injected into the servo controller to obtain the feedback signal. Subsequently, the feedback signal directly acted upon the GS to lock the transmission of E to the resonant longitudinal mode of the Ti:S laser. A 30-mm-long piezoelectric transducer (PZT) was adhered to M_3 to finely scan the cavity length to realize continuous frequency-tuning. To achieve a unidirectional operation of the single-frequency CW self-tuning Ti:S laser, a broadband retro-reflecting mirror (M_5) was placed in one arm of the output laser beam. Because the cavity contained only two optical elements, the total cavity length was only 333.5 mm.

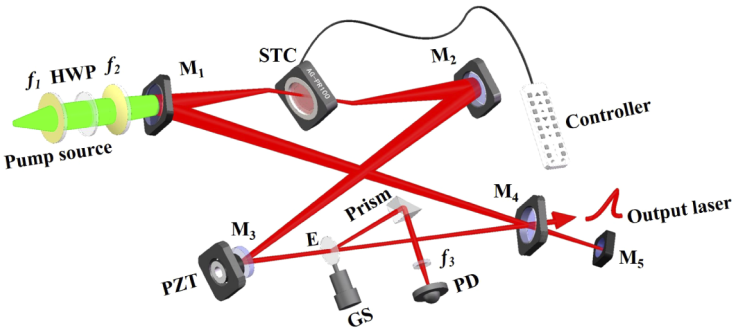

Fig. 4. Schematic diagram of designed Ti:S laser. HWP: half wave-plate; f_1 and f_2: coupling lenses; STC: self-tuning Ti:S crystal; PZT: piezoelectric transducer; E: etalon; GS: galvanometer scanner; PD: photodetector.

4. Experimental results

Before the E was inserted into the resonator, the tuning ability of the STC was first investigated. In this regard, a small portion of the output laser was injected into a grating spectrograph (Maya2000 Pro, Ocean Optics) to precisely record the operating wavelength of the self-tuning Ti:S laser. The obtained tuning curve is illustrated in Fig. 5, where the tuning angle φ between the optical axes and the incident plane was rotated from 0° to 90°. The tuning angle of 0° was the starting point of the STC rotation, i.e., both the optical axes and the polarization orientation of the pump laser were in the incident plane of the laser. The solid lines represent the theoretical predictions for interference orders k=8, 9, 10, and 11 of the STC. It was observed that no laser was emitted when the tuning angle varied from 0° to 6° (region A) and 64° to 90° (region D) owing to the large loss of the pump laser while tuning was performed in those regions. In the experiment, we observed that the pump laser with a maximum power of approximately 1.7 and 1.8 W was reflected by the STC in those regions. The observed phenomenon indicated that the pump laser was easily modulated by the rotating STC, consistent with a previous study [20]. Subsequently, by continuously rotating the STC from 6° to 30° (region B), the pump laser reflected from the STC gradually decreased and the laser began to emit, implying that in this case, the gain

Optics EXPRESS

of the laser began to exceed the loss. However, the laser wavelength fluctuated significantly when tuning was performed, owing to the weak undesired rejection of the STC in this region. Furthermore, the output laser wavelengths were tuned appropriately from 777.22 to 886.06 nm while the tuning angle of the STC was varied from 30° to 64°. In this case, the maximum tuning range and corresponding tuning slope efficiency were 108.84 nm and 3.2 nm/°, respectively. The tuning results obtained in this region were consistent with the theoretical prediction of k=10. Meanwhile, small plateaus were observed in the tuning curve for region C, attributable to pump power modulation.

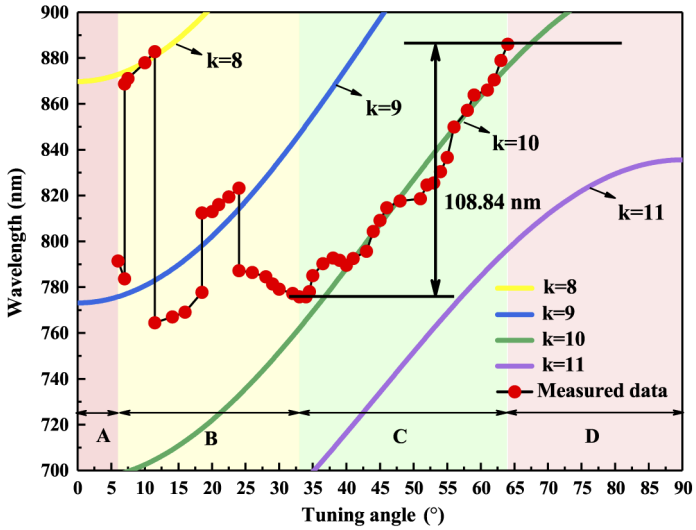

Fig. 5. Tuning curve of single-frequency CW self-tuning Ti:S laser as a function of tuning angle φ between optical axis and incident plane. Total thickness of STC was 8 mm.

For tuning region C, the output power corresponding to different wavelengths was further measured with a pump power of 11.5 W in the experiment, as shown in Fig. 6. A maximum output power of 1.38 W was achieved at an operating wavelength of 792.67 nm. With an increase in the operating wavelength of the self-tuning Ti:S laser, the output power decreased gradually. Furthermore, several power peaks were observed, revealing that the wavelength tuning of the self-tuning Ti:S laser was easily affected by the modulated pump power.

To investigate the optical conversion efficiency of the self-tuning Ti:S laser, the resonating wavelength was tuned close to approximately 795 nm, corresponding to the transition D_1 line of the Rb atom, by adjusting the angle between the optical axes and the incident plane to 41.5°. The output laser beam was injected into a power meter (PM30, Coherent Co., Ltd.) to record the output power. The experimental results are illustrated in Fig. 7. The minimum threshold of the pump power was 2.51 W, which was lower than that of the traditional single-frequency CW Ti:S laser (3.58 W) [14]. Furthermore, a maximum output power of 1.31 W was achieved under a pump power of 11.5 W. The nominal slope efficiency was 15.1%. In this case, the maximun power drained from M_2 was 4.65 W for the incomplete absorption of the pump laser caused by the limited thickness of the STC. This implies that the 1.31 W laser generated at 795 nm was owing to the 6.85 W incident pump power, and the corresponding slope efficiency measured as high as 30.2%, which was higher than that of the traditional single-frequency CW Ti:S laser (22%) [15]. The low threshold pump power and high slope efficiency should contribute primarily to the low intracavity insertion loss. In addition, owing to the absence of a traditional quartz BRF and an OD in this cavity, the cavity length was only 333.5 mm, i.e., only slightly longer than half the traditional single-frequency CW Ti:S laser (618 mm) [14]. The results revealed

Optics EXPRESS

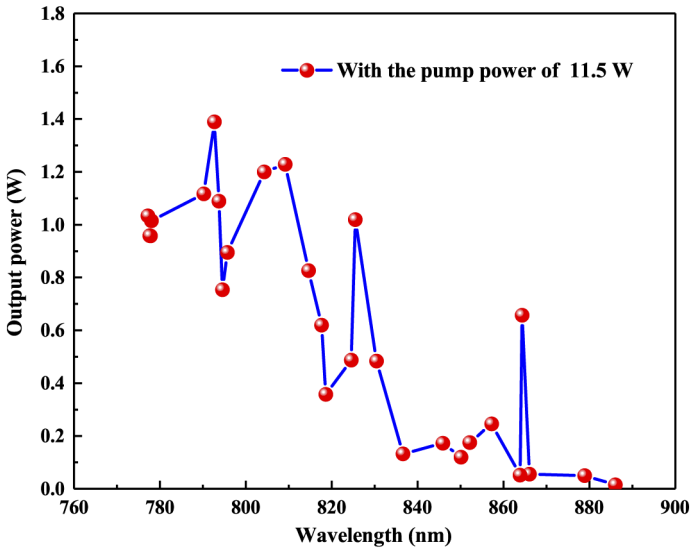

Fig. 6. Output power of single-frequency CW self-tuning Ti:S laser as a function of operating wavelength.

that the single-frequency CW-tunable Ti:S laser based on an STC is a promising method for effectively improving the efficiency of laser generation. In addition, the results provide a valuable reference for further improvement the power of single-frequency CW self-tuning Ti:S laser via the selection of a suitable doping concentration of STC.

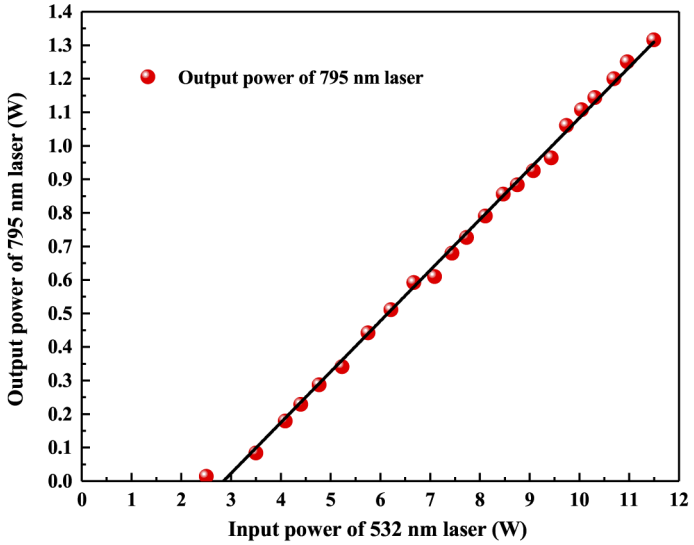

Fig. 7. Output power of free-running single-frequency CW self-tuning Ti:S laser with respect to pump power.

Additionally, we recorded the variations in the operating wavelength and corresponding full width at half maximum (FWHM) as we increased the pump power, as shown in Figs. 8(a) and 8 (b), respectively. When the pump power was increased from 3 to 11.5 W, clear blue shift was observed because the operating wavelength of the output laser shifted from 795.43 to 792.88 nm

Optics EXPRESS

and the FWHM was slightly broadened from 1.39 to 2.34 nm. These results implied that the optical path of the self-tuning Ti:S laser shortened with the increase in the pump power because of the severe thermal effect including the refraction index variation and the thermal lens focal length. Furthermore, because increasing the pump power can increase the gain of the Ti:S laser, more longitudinal modes began to oscillate in the resonator, resulting in the FWHM expansion of the laser spectrum. We focused more on the longitudinal mode structure of the self-tuning Ti:S laser. Hence, a scanning Fabry-Perot cavity with a free spectrum range of 750 MHz and finesse of 100, was employed in the experiment and the recorded curve is illustrated in Fig. 8(c). It was clear that several longitudinal modes oscillated simultaneously in the resonator and mode hopping occurred easily. To suppress multi-mode oscillation and mode-hopping, an E with a thickness and diameter of 1 and 10 mm, respectively, was inserted into the resonator. Using a direct-modulation locking system [26], E was well locked to the oscillating longitudinal mode of the self-tuning Ti:S laser. Consequently, a stable single-longitudinal-mode was achieved, as shown in Fig. 8(d).

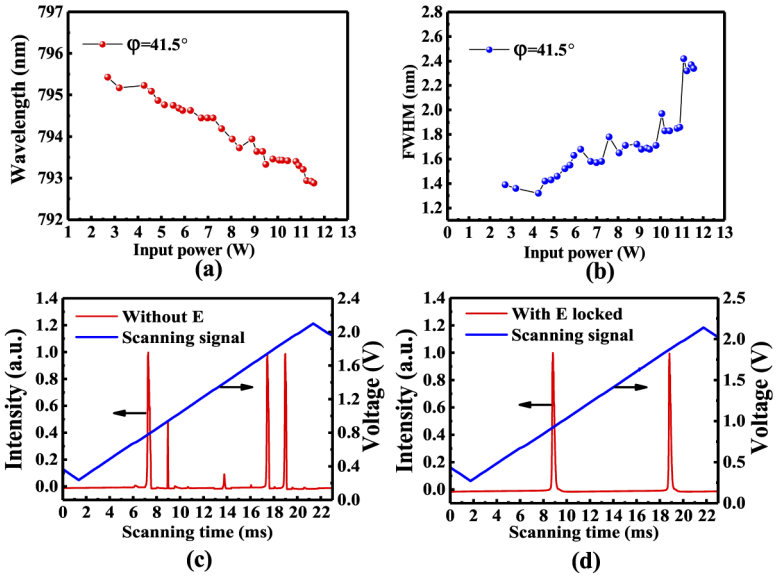

Fig. 8. Spectrum characteristics and longitudinal-mode structure of the self-tuning Ti:S laser. (a) variation of the operating wavelength, (b) FWHM variation, (c) longitudinal-mode structure before inserting the E, (d) longitudinal-mode structure after locking the E.

Subsequently, the beam quality of the generated laser was measured using an M^2 beam quality analyzer (M2SETVIS, Thorlabs), and the results are shown in Fig. 9. The M^2 values in the X- and Y-directions were M_x^2=1.03 and M_y^2=1.06, respectively. As shown in the inset of Fig. 9, the output laser beam closely resembled the standard Gauss distribution, which benefitted from the favorable astigmatism compensation by optimizing the cavity structure. Simultaneously, when the cavity was scanned by employing an intracavity PZT mirror as the single active element, the operating wavelength varied from 795.175 to 795.191 nm, and the recorded result is illustrated in Fig. 10. The maximum continuous frequency-tuning range was 9.95 GHz, which can precisely match the transition lines of alkali metal atoms and satisfy the requirements of atomic physics.

Finally, a small part of the leaked laser beam was partitioned equally into two parts with a power of 1 mW using a 50/50 beam splitter and then detected using a custom-developed balanced homodyne detector [27] to measure the intensity noise. The results are shown in Fig. 11. The noise spectra were measured from 0.2 to 5 MHz in our experiment. It was observed that the

Optics EXPRESS

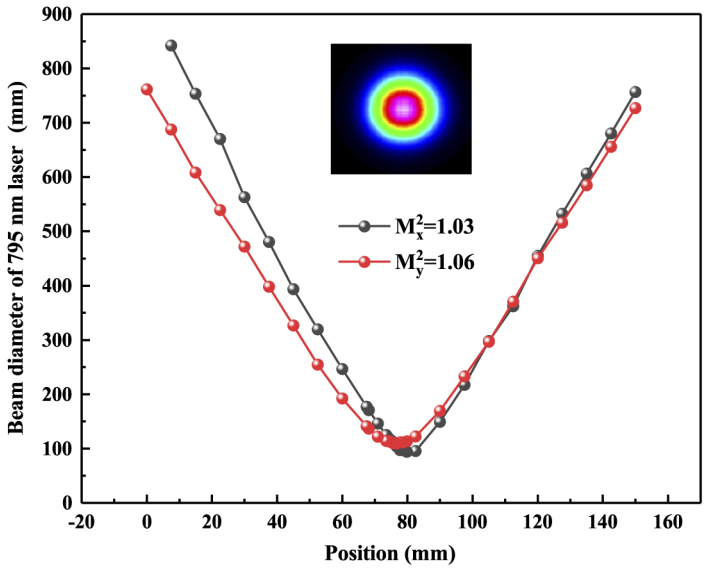

Fig. 9. Measured M^2 values and spatial beam profile of 795 nm laser.

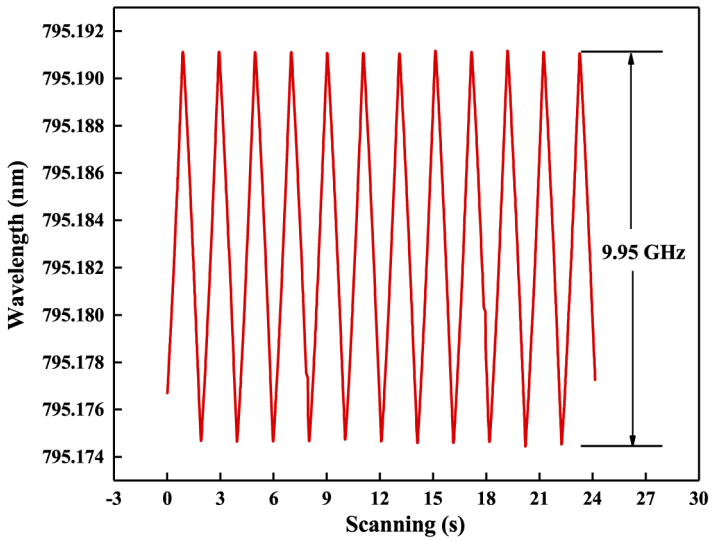

Fig. 10. Measured the maximum continuous frequency-tuning range of single-frequency CW self-tuning Ti:S laser.

measured frequency of the resonant-relaxation oscillation (RRO) peak was 973.2 kHz and the quantum noise limit (QNL) cut-off frequency was 2.09 MHz. It is noteworthy that the QNL cut-off frequency was lower than that of the traditional single-frequency CW tunable Ti:S laser (2.5 MHz) [28], which benefited from the short length of the designed STC, and the compact configuration of the cavity with low insertion loss. For the all-solid-state CW laser, the intensity noise was closely correlated with the stimulated emission rate of the coupling between atomic transitions and cavity modes, whereas the stimulated emission rate was proportional to the length of the gain medium. In the experiment, the length of the designed STC was much shorter than that of traditional 20-mm-long Ti:S crystal, thereby effectively decreased the stimulated emission

Optics EXPRESS

rate and resulted in low intensity noise in the obtained single-frequency CW self-tuning Ti:S laser.

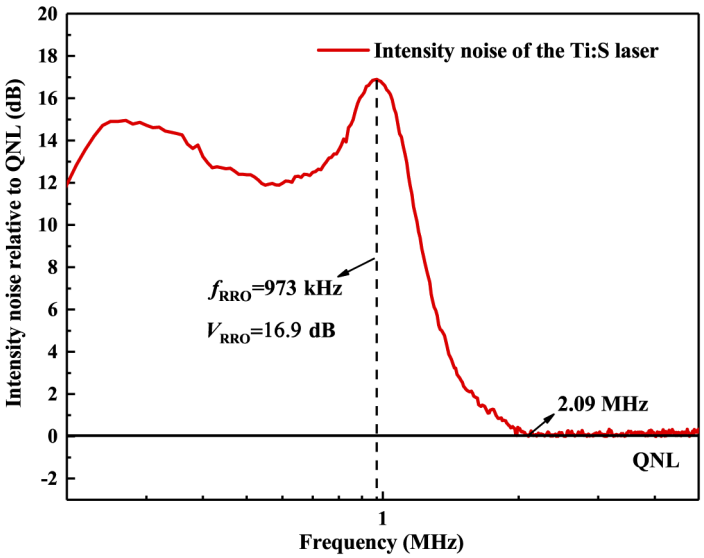

Fig. 11. Intensity noise of single-frequency CW self-tuning Ti:S laser.

5. Conclusions

In summary, we first realized a compact Watt-level single-frequency CW self-tuning Ti:S laser using a rotatable three-plate Ti:S crystal as both the gain medium and frequency-tuning element. The designed three-plate Ti:S crystal had a thickness ratio of 1:2:4, of which the thinnest plate was 1 mm. The optical axes were positioned on their own surfaces and parallel to each other. Because the resonator contained only two optical elements, the cavity length measured only 333.5 mm, i.e., only slightly longer than half the traditional single-frequency CW Ti:S laser. In the experiment, by optimizing the resonator structure, a maximum wavelength tuning range of 108.84 nm was experimentally achieved, consistent with theoretical prediction. When the laser wavelength was tuned to 795 nm, a maximum output power of 1.31 W and a corresponding slope efficiency of 30.2% were obtained. The experimental results showed that the high output power and conversion efficiency benefited from the low insertion loss. After an inserted E was locked to the resonant longitudinal mode of the resonant cavity, the stable single-longitudinal-mode of the output laser was successfully realized. Additionally, the output characteristics of the obtained single-frequency self-tuning Ti:S laser were measured. The M^2 values in the X- and Y-directions were M_x^2=1.03 and M_y^2=1.06, respectively. A maximum continuous frequency-tuning range of 9.95 GHz was achieved by employing an intracavity PZT mirror as the single active element. The measured frequency of the RRO peak and the QNL cut-off frequency were 973.2 kHz and 2.09 MHz, respectively. In general, the experimental results revealed that the obtained compact Watt-level single-frequency CW self-tuning Ti:S laser with perfect beam quality, broad continuous frequency-tuning range, and low intensity noise can provide a high-quality laser source for quantum optics. The cavity structure was effectively simplified in the study, thereby providing a foundation for the miniaturization of an all-solid-state single-frequency CW-tunable Ti:S laser.

Funding. National Natural Science Foundation of China (62027821, 61975100); National Key Research and Development Program of China (2016YFA0301401); Key Research and Development Program of Shanxi Province

Optics EXPRESS

(201903D111001); Fund for Shanxi "1331 Project" Key Subjects Construction; Program for the Innovative Talents of Higher Education Institution of Shanxi.

Disclosures. The authors declare no conflicts of interest.

References

1. Y. Sun, H. D. Lu, and J. Su, "Continuous-wave, single-frequency, all-solid-state Ti:Al_2O_3 laser," Acta Sin. Quant. Opt. **14**(3), 344–347 (2008).
2. P. F. Moulton, "Spectroscopic and laser characteristics of Ti:Al_2O_3," J. Opt. Soc. Am. B **3**(1), 125–133 (1986).
3. T. Kuwanmoto, K. Honda, Y. Takahashi, and T. Yabuzaki, "Magneto-optical trapping of Yb atoms using an intercombination transition," Phys. Rev. A **60**(2), R745–R748 (1999).
4. Z. X. Xu, W. Y. Wu, L. Tian, L. R. Chen, Z. Y. Zhang, Z. H. Yan, S. J. Li, and H. Wang, "Long lifetime and high-fidelity quantum memory of photonics polarization qubit by lifting zeeman degeneracy," Phys. Rev. Lett. **111**(24), 240503 (2013).
5. X. J. Jia, Z. H. Yan, Z. Y. Duan, X. L. Su, H. Wang, C. D. Xie, and K. C. Peng, "Experimental realization of three-tolor entanglement at optical fiber communication and atomic storage wavelengths," Phys. Rev. Lett. **109**(25), 253604 (2012).
6. F. Wolfgramm, A. Cere, F. A. Beduini, A. Predojevic, M. Koschorreck, and M. W. Mitchell, "Squeezed-light optical magnetometry," Phys. Rev. Lett. **105**(5), 053601 (2010).
7. A. Sanchez, R. E. Fahey, A. J. Strauss, and R. L. Aggarwal, "Room-temperature continuous-wave operation of a Ti:Al_2O_3 laser," Opt. Lett. **11**(6), 363–364 (1986).
8. P. A. Schulz, "Single-frequency Ti:Al_2O_3 ring laser," IEEE J. Quantum Electron. **24**(6), 1039–1044 (1988).
9. G. T. Maker and A. I. Ferguson, "Ti:sapphire laser pumped by a frequency-doubled diode-pumped Nd:YLF laser," Opt. Lett. **15**(7), 375–377 (1990).
10. http://www.m2lasers.com/lasers/all-lasers/solstis-ti-sapphire-lasers.aspx.
11. http://www.coherent.com/Products/index.cfm?846/MBR-Ring-Series.
12. http://www.spectra-physics.com/products/tunable-lasers/matisse.
13. S. M. Kobtsev, V. I. Baraulya, and V. M. Lunin, "Combined cw single-frequency ring dye/Ti:sapphire laser," Quantum Electron. **36**(12), 1148–1152 (2006).
14. X. J. Sun, J. Wei, W. Z. Wang, and H. D. Lu, "Realization of a continuous frequency-tuning Ti:Sapphire laser with an intracavity locked etalon," Chin. Opt. Lett. **13**(7), 071401 (2015).
15. P. X. Jin, H. D. Lu, Y. X. Wei, J. Su, and K. C. Peng, "Single-frequency CW Ti:sapphire laser with intensity noise manipulation and continuous frequency-tuning," Opt. Lett. **42**(1), 143–146 (2017).
16. Y. X. Wei, H. D. Lu, P. X. Jin, and K. C. Peng, "Self-injection locked CW single-frequency tunable Ti:sapphire laser," Opt. Express **25**(18), 21379–21387 (2017).
17. J. Fernandez, I. Iparraguirre, I. Aramburu, A. Illarramendi, J. Azkargorta, and M. Voda, "$K_5Nd(MoO_4)_4$: a self-tunable laser crystal," Opt. Lett. **28**(15), 1341–1343 (2003).
18. J. Fernandez, M. A. Illarramendi, I. Iparraguirre, I. Aramburu, J. Azkargorta, M. Voda, M. Al-Saleh, and R. Balda, "$Rb_5Nd(MoO_4)_4$ a self-tunable birefringent laser crystal," Opt. Mater. **26**(4), 483–487 (2004).
19. I. Aramburu, I. Iparraguirre, M. A. Illarramendi, J. Azkargorta, J. Fernandez, and R. Balda, "Self-tuning in birefringent $La_3Ga_5SiO_{14}:Nd^{3+}$ laser crystal," Opt. Mater. **27**(11), 1692–1696 (2005).
20. I. Iparraguirre, I. Aramburu, J. Azkargorta, M. A. Illarramendi, J. Fernandez, and R. Balda, "Wavelength tuning of Titanium Sapphire Laser by its own crystal birefringence," Opt. Express **13**(4), 1254–1259 (2005).
21. I. Iparraguirre, J. Azkargorta, J. Fernandez, R. Balda, T. Gatelurrutia, M. A. Illarramendi, and I. Aramburu, "A self-tunable Titanium Sapphire Laser by rotating a set of parallel plates of active material," Opt. Express **17**(5), 3771–3776 (2009).
22. X. L. Wang and J. Q. Yao, "Transmitted and tuning characteristics of birefringent filters," Appl. Opt. **31**(22), 4505–4508 (1992).
23. Q. W. Yin, H. D. Lu, and K. C. Peng, "Investigation of the thermal lens effect of the TGG crystal in high-power frequency-doubled laser with single frequency operation," Opt. Express **23**(4), 4981–4990 (2015).
24. C. W. Zhang, H. D. Lu, Q. W. Yin, and J. Su, "Continuous-wave single-frequency laser with dual wavelength at 1064 and 532 nm," Appl. Opt. **53**(28), 6371–6374 (2014).
25. W. Z. Wang, H. D. Lu, J. Su, and K. C. Peng, "Broadband tunable single-frequency Nd:YVO_4/LBO green laser with high output power," Appl. Opt. **52**(11), 2279–2285 (2013).
26. F. Q. Li, B. Zhao, J. Wei, P. X. Jin, H. D. Lu, and K. C. Peng, "A continuously tunable single-frequency 455 nm blue laser for high-state excitation transition of cesium," Opt. Lett. **44**(15), 3785–3788 (2019).
27. Y. R. Guo, W. N. Peng, J. Su, H. D. Lu, and K. C. Peng, "Influence of the pump scheme on the output power and the intensity noise of a single-frequency continuous-wave laser," Opt. Express **28**(4), 5866–5874 (2020).
28. H. D. Lu, J. Su, C. D. Xie, and K. C. Peng, "Experimental investigation about influences of longitudinal-mode structure of pumping source on a Ti:Sapphire laser," Opt. Express **19**(2), 1344–1353 (2011).

183.191.160.58 {ts '2021-01-14 17:40:05'}